

Performance of an innovative direct-push piston sampler in soft clay

Jubert A. Pineda

ARC Centre of Excellence for Geotechnical Science and Engineering, The University of Newcastle, Australia

Allan McConnell

Managing Director, In-situ Geotech Services (IGS), Australia

Richard B. Kelly

ARC Centre of Excellence for Geotechnical Science and Engineering, The University of Newcastle, NSW, Australia

ABSTRACT: An innovative direct-push sampler has been developed to maximize sample retention and reduce disturbance. The stainless steel sampler has an outer diameter of 63mm, a wall thickness of 1.6mm and a toe cutting angle of 5 degrees. The sampler is inserted into the ground by direct push methods, then operates as a conventional fixed-piston sampler until it is about to be withdrawn from the ground. Prior to withdrawal a very brief “shot” of pressurized nitrogen is injected horizontally at the base of the sample, just above the cutting edge, to cut the soil. Then, during withdrawal, low pressure air or water is injected into the void that develops below the sampler to overcome the suction that otherwise would develop as it is pulled out of the ground. Sample quality is investigated in this paper, using CAT scans performed on each of the samples prior to extrusion, constant rate of strain compression and triaxial tests

1 INTRODUCTION

This paper describes the performance of an innovative direct-push piston sampler specifically designed to reduce sample disturbance and maximize sample retention. The sampler’s performance for testing soft clays is described. Laboratory tests as well as CAT scans have been used to evaluate the reliability of the sampler and also to estimate sample disturbance.

2 SAMPLER DESCRIPTION AND OPERATION PRINCIPLE

The device is a piston-pneumatic-injection (PPI) sampler specifically designed to maximize sample retention and reduce sample disturbance. The stainless steel sampling tube has an outer diameter of 63mm, length of 880mm a wall thickness of 1.6mm and a 5 degree cutting edge. The area ratio is 11% with no inside clearance. The operation principle is schematically shown in Figure 1. The tube is closed using a conical fixed piston inside of the tube during advancement into the soil to the top level of the sampling depth. Advancement to sampling depth is made by direct pushing using a CPT rig in a similar fashion to pushing a CPT. The piston is then held stationary as the tube is advanced 880mm into the soil to capture the sample. The sampling tube is advanced over the stationary fixed piston using a specially-designed cylinder behind the tube, actuated by water pressure of approximately 100 bar. The sample in the tube is released from the soil mass below by “cutting” it free with a very brief injection (a “shot”) of high pressure (70 bar) nitrogen at the sample tube cutting face, before it is extracted. Two stainless steel tubes (6mm in diameter) externally welded to the sampling tube are used to apply the nitrogen directly below

the cutting face. As the sample tube is extracted, low pressure air or water is injected into the void below the sampler, to eliminate suction while pulling out. The objectives of this procedure are to reduce tension in the sample and to avoid sample loss due to suction. The tube is then unscrewed and pulled off the piston. However, this version of the sampler does not have a pressure release grub screw in the piston and suctions are generated between the sample and the piston when removing the tube from the piston.

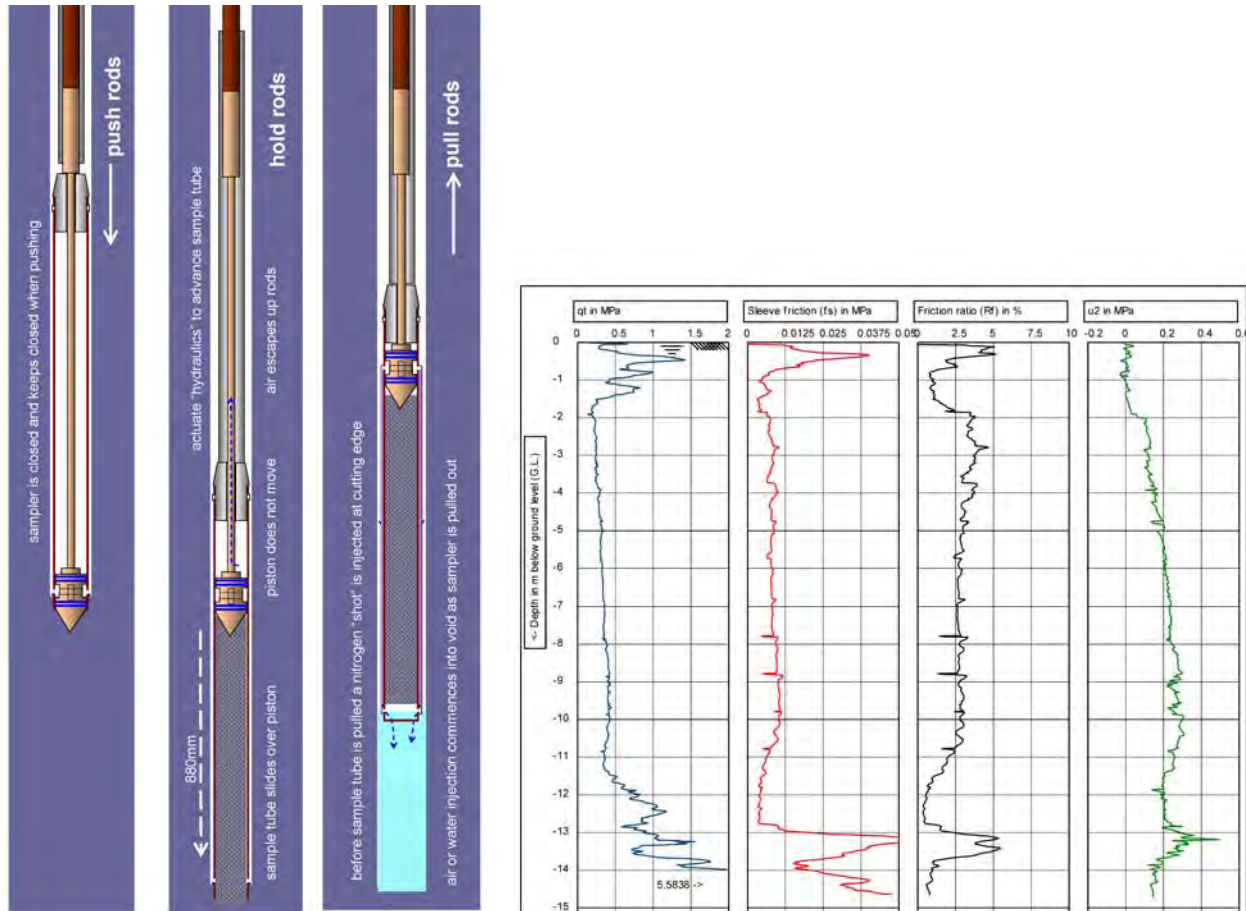


Figure 1 (a) Operation of the piston sampler. (b) CPTu profile at Ballina site

3 SITE DESCRIPTION AND SAMPLING PROGRAM

The new PPI sampler has been recently employed for sampling soft estuarine deposits from the Richmond River valley in northern New South Wales (Australia). The sampling program was carried out at the recently established national field testing facility for soft soils, near Ballina (NSW) (Kelly, 2013). The soil sampled, hereafter Ballina clay, represent these complex Holocene age estuarine deposits frequently related to local settlement and stability problems. In general terms, the soil profile comprises an upper alluvium layer ($\approx 1.5\text{m}$ thick) overlying a 10m thick soft estuarine clay layer. The water table is located close to the ground surface (near sea level). The clay fraction is mainly composed of smectite, kaolinite and mica/illite with variable percentages and has an organic content of 5% (Bishop, 2010).

The sampling program was carried out at two locations in close proximity, IGS-S1 and IGS-S2. PPI samples were retrieved at intervals of 1m until a maximum depth of 10m. The PPI sampler used at IGS-S2 was coated internally with a non-stick coating, to assess if that enhanced sampler performance. The performance of both versions of the new sampler is evaluated here by comparing the preliminary results

from laboratory tests and CAT-scans, for a representative depth defined at $-7.5 < z < -8.4\text{m}$. Figure 1b shows a CPTu profile traced before sampling close to the locations where the PPI samples were taken.

4 TESTING PROGRAM

The laboratory testing program combined Computerized Axial Tomography (CAT), used as a non-destructive technique to examine the soil quality prior to testing, and a laboratory program that included: (i) characterization tests: Atterberg limits, natural water content and density of solid particles, (ii) one-dimensional consolidation tests with shear wave velocity measurements, V_s , using bender elements transducers (CRS+BE), and (iii) triaxial compression tests (CKoU).

Each tube was sliced horizontally before sample trimming with the aim to minimize the adhesion force at the clay-tube interface during soil extrusion. An angle grinder was used to slice the stainless steel tube and afterwards a wire saw was used to cut the clay. Specimens for oedometer and triaxial testing were trimmed from 45mm-thick and 140mm-thick slices, respectively. For each tube, the location of tested specimens is shown in Figure 2. The experimental tests reported in this paper were carried out by keeping constant the natural electrical conductivity of the soil pore fluid due to their important influence on the clay behaviour (e.g., Pineda et al, 2013). The electrical conductivity (EC) of the natural pore water was determined by squeezing out the soil pore water using a stainless steel compaction mold. The upper 50mm-thick slice of soil, commonly highly disturbed by the sampling process, was used for this purpose. Then, a synthetic salt solution was prepared by mixing deionized water with the required mass of sodium chloride. Natural EC ranged around 35-37mS/cm. Based on this, a synthetic salt solution, $EC \approx 37.1\text{mS/cm}$, was prepared and used in laboratory tests (both CRS and TXR tests).

5 CAT SCANS

CAT scans were used to examine the internal structure of the tube samples. Particular emphasis focused on the detection of possible heterogeneities (e.g., shells, fissures, cavities, etc), and their potential influence on laboratory testing, due to the complex geological environment in which Ballina clay was formed. The CAT analysis was performed in collaboration with the Radiology Section of the Mater Hospital in Newcastle (NSW). A CAT scanner (Toshiba Aquilion®) with 135keV maximum energy was used. Image post processing used the free software Gimias® (Gimias, 2011).

Figure 2 shows the vertical sections of the tube samples IGS-S1 and IGS-S2, retrieved using the new sampler. The attenuation scale varies from white (maximum attenuation or high material density) to black (minimum attenuation or low density). CAT images obtained on a tube sample retrieved at the same depth using a standard U75 Shelby tube sampler (75mm diameter, 1.6mm wall thickness) has been also included for comparison. The inspection of Figure 2 clearly shows a loss of resolution for the CAT profiles from IGS-S1 and IGS-S2 due to the interference of the two external stainless steel tubing –high attenuation- used to cut the soil base. Some sub-horizontal cracks were observed in the IGS samples at the upper part of the tube. It was clearer for IGS-S1 and may be attributed to the suction created during pulling out the piston. A larger area of sub-horizontal cracking was observed in the U75 sample. The presence of shells, indicated as white inclusions, is also evident in all cases. From a qualitative viewpoint, the upper half of the IGS samples shows a quite homogeneous soil layer. However, the changes in the grey intensity observed at the upper zone of the bottom half of both IGS samples (clearer in IGS-S1) suggest a reduction in soil density. The profile of the U75 sample shows that cracks are distributed along the whole tube. Only the upper part of the IGS tubes can be compared against U75 tube due to their shorter length.

Figure 2 also shows cross-section images obtained at different depths along the tube for all the three samples scanned. There, capital letters F, C and S stands respectively for fissure/heterogeneity, cavity/channel and shell. The influence of the two external tubes on the quality of the CAT images from IGS sampler is clearly identified by the narrow and distorted zone crossing the sample in all the images. In general, fissures of variable thickness are observed along the tubes that suggest some vertical connec-

tivity between them. This behaviour is even more evident in the U75 sample where, open-wide fissures and cavities can be detected at different levels. For IGS samples, the presence of fissures reduced at the central part of the tube that is also consistent with the reduction of the fissuring pattern observed in the U75 sample. Shells of variable size are observed in all the three tubes. In the case of IGS-S1, the trimming process for specimen CRS 2 was not possible due to the presence of shells (see Figure 2). Based on the visual qualitative evidence obtained from CAT-scans it seems that the new sampler induces lower sampler disturbance, at least in terms of the fissuring pattern, than the standard U75 open sampler despite its smaller diameter.

6 MATERIAL CHARACTERIZATION

Material characterization was performed on representative samples from both IGS-S1 and IGS-S2. Liquid limit Fall Cone test (LL) and plasticity index (PI) were determined according to AS1289.3.9.1 and AS1289.3.2.1, respectively. Density of the solid particles, ρ_s , was obtained from gas pycnometer tests. Results are summarized in Table 1 where the initial conditions of specimens used for CRS and TXR testing are also included for comparison.

Average values for liquid limit and plasticity index were around 125% and 40%, respectively. The fine fraction classified (USCS) as a high plasticity clay (CH). The density of solids, ρ_s , ranged around 2.70 Mg/m^3 . The natural water content (w) along the upper half tubes reduced consistently with depth. Some scatter was observed in the maximum water content (112% for IGS-S1 and 106% for IGS-S2) whereas small scatter was observed for specimens located at the middle part of the tube in both cases ($\approx 93\%$). Initial void ratio (e) (and dry density, ρ_d) varied in agreement with the water content from 3.03 to 2.48. In all cases, full saturation of the specimens was inferred (S_r).

Table 1. Index properties and initial conditions of samples tested

Tube	Reference	EC (mS/cm)	Atterberg limits*		ρ_s (Mg/m ³)	w (%)	ρ_d (Mg/m ³)	e	S_r
			LL (%)	PI (%)					
S1	CRS 1	35.1	125.4	30.2	2.70	112.72	0.67	3.03	1.00
	CRS 2					103.05	0.71	2.82	0.99
	TXR 2					92.23	0.78	2.48	1.00
S2	CRS 1	37.1	136.7	35.4	2.70	102.9	0.71	2.78	1.00
	CRS 2					105.6	0.70	2.85	1.00
	TXR 2					93.22	0.76	2.54	0.99

* Tests performed on the clay fraction ($<425\mu\text{m}$) by using a synthetic solution at the same EC as the natural clay

7 OEDOMETER TESTS

The compressibility of Ballina clay was studied by means of Constant Rate of Strain (CRS) tests equipped with bender elements. The CRS equipment used a thin stainless steel oedometric ring ($\phi_{\text{int}} = 48\text{mm}$, $h = 20\text{mm}$, $t = 1\text{mm}$, corresponding to an area ratio of 9%) to retrieve samples following the experimental procedure described by Pineda et al. (2012). Excess pore-water pressure is measured at the sample bottom whereas the upper drainage outlet is maintained at atmospheric conditions during loading. The shear wave velocity was determined using the method of Viggiani & Atkinson (1995)

CRS tests were performed on four specimens, two from each tube, as indicated in Figure 2. The main properties of samples tested are summarized in Table 1. CRS tests consisted of three stages: (i) saturation, (ii) loading, and (iii) unloading. Despite the initial saturation of the samples, they were subjected to a 48 hr saturation stage under constant vertical total stress ($\sigma_v \approx 19\text{kPa}$) and water-back pressure ($u_w \approx 10\text{kPa}$). After that, the specimens were loaded under a constant rate of strain equal to $0.004\%/min$. The same strain rate was applied during unloading. The maximum vertical effective stress was around $500\text{--}550\text{kPa}$.

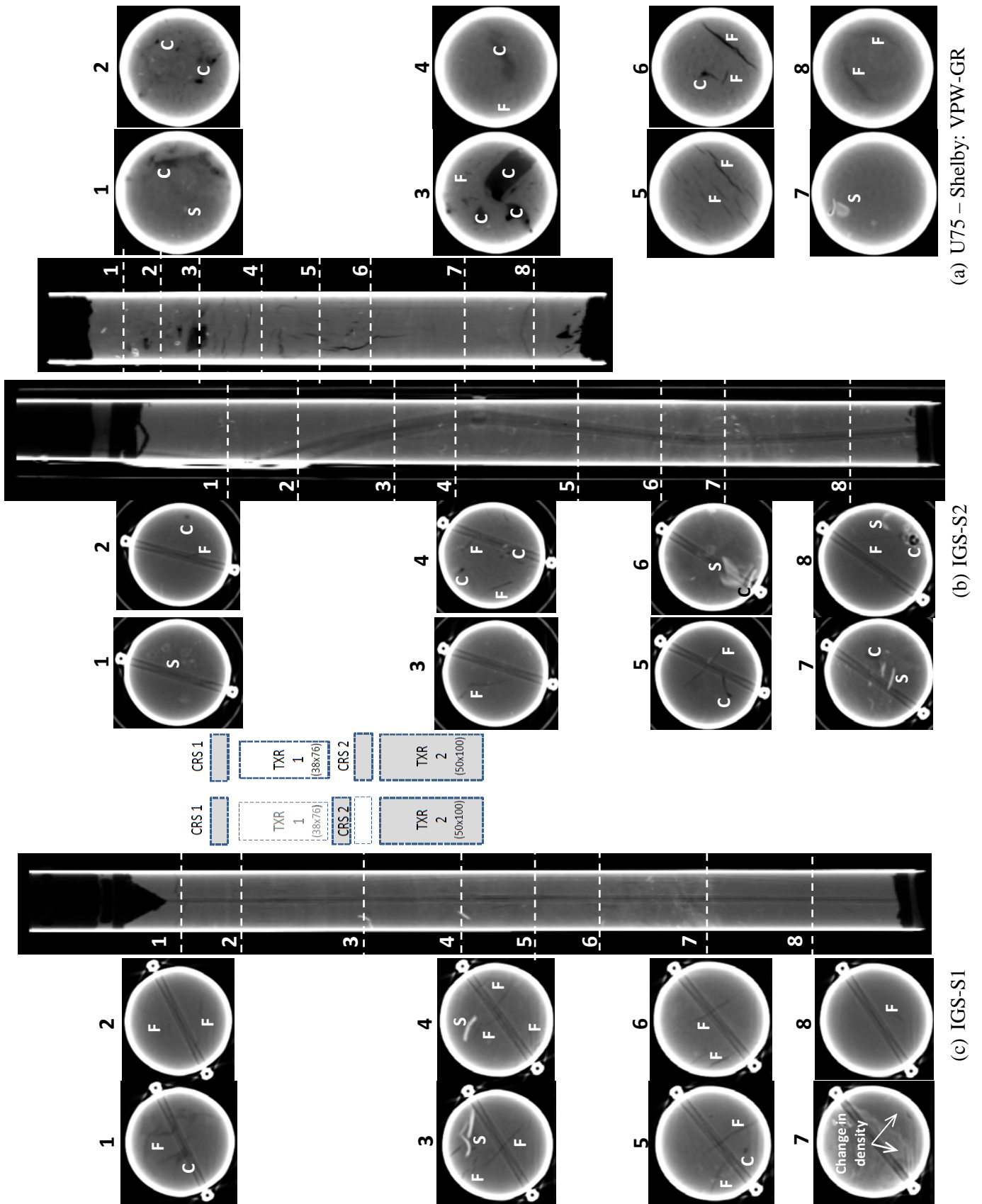


Figure 2. Cross-section CT images. (a) IGS S1. (b) IGS S2. (c) U75: VPW_GR. (*F*: fissure/heterogeneity; *S*: shell; *C*: cavity/channel)

Figure 3(a) shows the evolution of volumetric strain and pore-water pressure during the loading-unloading path for the four samples tested. Similar stress-strain behaviour was obtained for all samples tested. The in-situ vertical effective stress at sample depth was estimated from bulk densities and the position of the water table ($\sigma'_{v(\text{in-situ})} \approx 50\text{kPa}$) indicated as a vertical dashed line in Figure 3. The volumetric strain at $\sigma'_{v(\text{in-situ})}$ ranged between 2.6-3.0% and 1.6-2.5% for specimens from IGS-S1 and IGS-S2, respectively.

Figure 3(b) shows the compressibility curves obtained from the CRS tests. The non-linear nature of the compressibility curve of Ballina clay can be seen in Figure 3. Compressibility parameters C_c and C_s were used to determine the Cam-Clay parameters λ and κ as shown in Table 2. Preconsolidation pressure, σ'_{prec} , was determined using the strain-energy method (Becker et al, 1987) and ranged between 65-76kPa to 67-71kPa for specimens from IGS-S1 and IGS-S2, respectively. Values of σ'_{prec} are indicated in Figure 3(b) by grey squares. The estimated OCR ranged between 1.3-1.52 and 1.34-1.42, respectively. The evolution of the shear wave velocity, V_s , during loading showed a bi-linear response. A small increase was observed at values of effective stress around $\sigma'_{v(\text{in-situ})}$. There, V_s ranged from 59-62 to 62-66m/s. These values are in agreement with results from a nearby SMDT test. At that depth, the shear wave velocity from SDMT was $V_{s(\text{SDMT})} \approx 60\text{m/s}$. V_s increased almost linearly with σ'_v for values higher than 65-75kPa. That range of stress is similar to the estimated preconsolidation stresses described above and also seems to be consistent with the observed inflection point in the pore water pressure response during loading (see Figure 3(a)). Table 2 summarizes the results obtained from CRS tests.

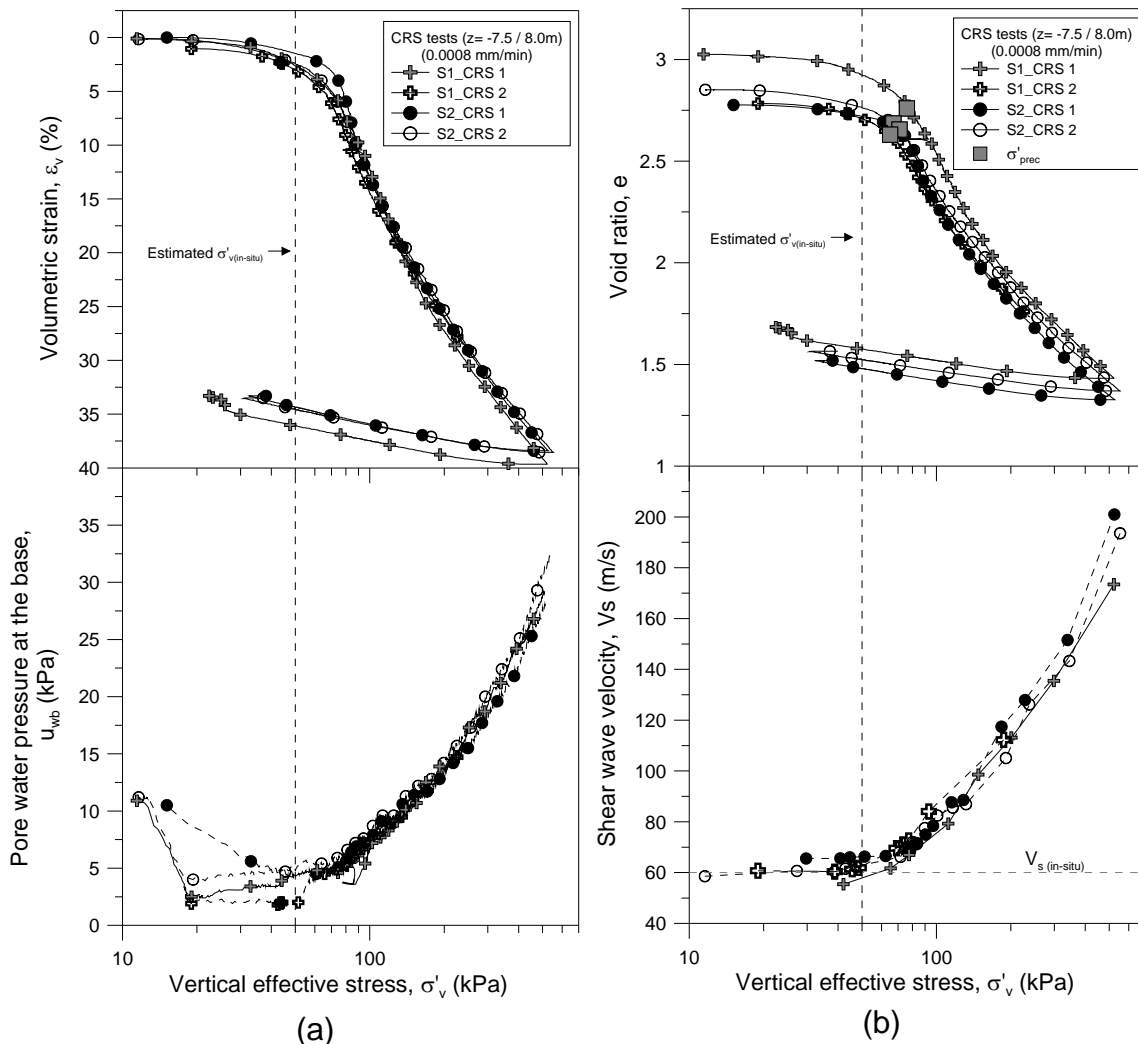


Figure 3. CRS tests. (a) evolution of volumetric strain and pore water pressure during loading. (b) oedometric curves and evolution of the shear wave velocity.

Table 2. Results from CRS tests

Tube	Test	$\sigma'_{prec} < \sigma'_v < 150 \text{ kPa}$		$\sigma'_v > 200 \text{ kPa}$		C_s	κ	σ'_{prec} (kPa)	OCR	V_s at $\sigma'_{v(in-situ)}$ (m/s)
		C_c	λ	C_c	λ					
S1	CRS 1	2.18	0.95	1.24	0.54	0.19	0.08	76	1.52	59
	CRS 2	1.83	0.80	1.23	0.53	-	-	65	1.30	62
S2	CRS 1	1.57	0.68	1.10	0.48	0.18	0.08	71	1.42	66
	CRS 2	1.67	0.72	1.16	0.50	0.17	0.07	67	1.34	62

8 STRENGTH TESTS

Anisotropic triaxial compression tests (CKoU) were performed to study the stress-strain behaviour of Ballina clay. The results of two triaxial tests –TXR2–, one from each tube and both located at similar depths, are presented here (see Table 2 and Figure 2). Tested specimens (50mm in diameter and 100mm height) were trimmed using a soil lathe. The tests were performed in a stress-path triaxial system (Imperial College, London) and consisted of three stages: (i) saturation, (ii) anisotropic consolidation, and (iii) shearing under undrained conditions. A stress-controlled saturation ramp was applied until achieve values of cell pressure and back water-pressure equals to 510 and 505kPa, respectively ($\sigma'_r = 5\text{kPa}$). After 48hrs of equalization, Skempton's parameter B was around 0.98. Anisotropic consolidation followed the corresponding value of K_0 for depths between 7.5-8.0 m. Values of K_0 ranging between 0.44 and 0.48 were estimated from the SDMT test. Specimens from IGS-S1 and IGS-S2 followed, respectively, K_0 values of 0.46 and 0.43. An axial stress rate of 6 kPa/day, equivalent to an axial strain rate of $\dot{\epsilon} \approx 0.5\% / \text{day}$, was adopted during consolidation. At the end of the consolidation stage, the specimen from IGS-S1 reached an axial stress similar to the in-situ vertical effective stress ($\sigma'_{a(S1)} \approx \sigma'_{v(in-situ)} = 51.5\text{kPa}$). The specimen from IGS-S2, on the other hand, was allowed to exceed the estimated in-situ vertical stress by 8kPa ($\sigma'_{a(S2)} = 58.5\text{kPa}$) but without surpassing the preconsolidation stress reported in Figure 4(b). Finally, each sample was subjected to axial compression under undrained conditions until reach a maximum axial strain around 20%. An axial strain rate equal to 5%/day was used.

Figure 4(a) shows the evolution of void ratio, e , with the mean effective stress, p' , during the anisotropic consolidation stage. Specimen from IGS-S2 experienced a higher reduction in void ratio before reaching the strain criterion adopted here for ending the consolidation process, that was due to the higher initial void ratio and the slight increase in the maximum stress applied despite the preconsolidation stress not being exceeded. Figure 4(b) shows the stress-strain curves obtained during the shearing stage. The excess of the pore water pressure during shearing is also included. Pore water pressure showed positive values along the whole shearing stage. Similar values were recorded in both samples with a maximum around 17kPa. The peak deviatoric stress was achieved at axial strains lower than 1% in both specimens. The maximum deviatoric stress, q_{peak} , was similar in both specimens (42.3 and 44.8kPa for specimens from IGS-S1 and IGS-S2, respectively). The undrained shear strength obtained from the triaxial tests ($S_u = q_{peak}/2$) was in agreement with the results obtained from CPTU tests at depths between 7.5 - 8.0m "calibrated" to shear vane data using $N_{kt} = 13$ ($S_{u(CPTU)} \approx 20\text{kPa}$). Sample buckling was observed in specimen from IGS-S1 at an axial strain around 1.5%. The presence of shells, as observed in Figure 3, seemed to be the main reason for sample buckling that affected the failure mode.

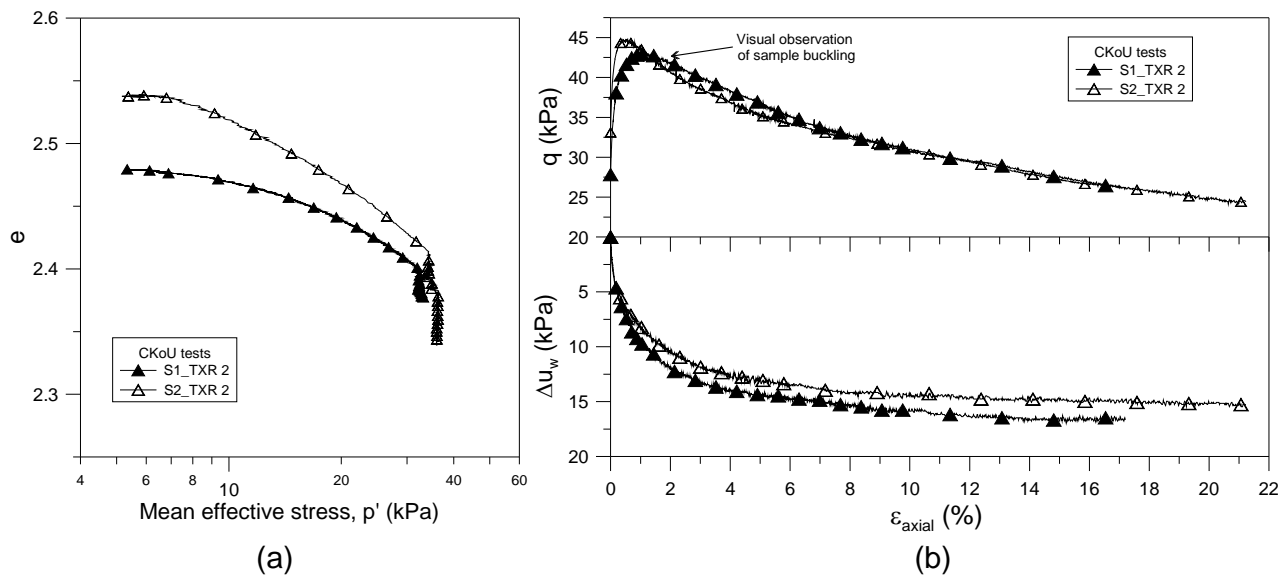


Figure 4. Triaxial tests. (a) Consolidation stage. (b) Shearing stage.

9 SAMPLE DISTURBANCE

Sample disturbance is a concern when testing soft soils. Lunne et al (1997) proposed a method where the change in void ratio (Δe) at in-situ stress ($\sigma'_{in-situ}$) is normalized by the initial void ratio value ($\Delta e/e_0$). Four levels of sample quality are specified from *very good to excellent* ($\Delta e/e_0 < 0.04$), *good to fair* ($0.04 < \Delta e/e_0 < 0.07$), *poor* ($0.07 < \Delta e/e_0 < 0.14$) and *very poor* ($\Delta e/e_0 > 0.14$). Table 3 summarizes the analysis of sample disturbance according to the Lunne et al (1997) criterion by using the results from both CRS and triaxial tests described above.

Following the Lunne et al (1997) criteria, the quality of triaxial specimens classified as *good to fair* irrespective from their origin (IGS-S1 or IGS-S2). Specimens used for CRS tests showed a quality *very good to excellent* in all cases. A close inspection of values presented in Table 3 indicates that CRS specimens from IGS-S2 developed smaller volumetric compression in order to reach to the in-situ stress. The influence of shells on the compressibility of the triaxial specimen from IGS-S1 is not straightforward to evaluate at this stage. Further experimental data are required to clarify this aspect.

The comparison of the shear wave velocity from laboratory tests against values obtained in-situ indicates a small change in the soil structure induced by sampling. From these preliminary results the velocity ratio, $V_{s(lab)}/V_{s(SDMT)}$, suggest that specimens from IGS-S2 were subjected to some additional compression (overconsolidation) during sampling. For these samples, $V_{s(lab)}$ increased between 3 to 9%. The reduction in $V_{s(lab)}$ in specimens from IGS-S1 was around 3%. The apparent increase in overconsolidation may be due to the nitrogen cutting pressure and suction on tube removal from the piston being transferred to the soil better due to the low adhesion coating. Subsequent consolidation within the sample would lead to a local increase in overconsolidation. For this to occur there must be areas within the tube associated with swelling and the CT scans suggest that swelling may have occurred in the lower portion of the tubes leading to a reduction in density.

ISSMFE (1981) suggested that the shear strain at peak deviator stress could be used as an indicator of soil disturbance. Typically high quality samples have a small strain to failure and a well defined peak shear stress. As the sample becomes more disturbed the strain to failure increases and the peak shear stress becomes less well defined. The data showed in Figure 4b indicates that the strain to failure is less than 1% and that there is a well defined peak shear stress. Qualitatively this indicates that there is not a great deal of disturbance affecting these samples. Further strength tests are being planned on samples taken from a variety of tube and piston samplers to enable quantitative comparisons of strain to failure and peak shear strength to be made.

Table 3. Evaluation of sample disturbance.

Tube	Test	ε_{vol} at σ'_v (in-situ) (%)	e at σ'_v (in-situ)	$\Delta e/e_0$	Sample quality*	$V_{s(lab)}$ at σ'_v (in-situ) (m/s)	$V_{s(lab)}/V_{s(SMDT)}$	ε_s at q_{peak} (%)
IGS-S1	CRS 1	2.60	2.92	0.035	Very good to excellent	58	0.97	N/A
	CRS 2	3.00	2.71	0.040	Excellent / Good to fair	62	1.03	N/A
	TXR 2	2.95	2.38	0.041	Good to fair*	N/A	N/A	0.81
IGS-S2	CRS 1	1.60	2.72	0.022	Very good to excellent	66	1.09	N/A
	CRS 2	2.50	2.76	0.032	Very good to excellent	62	1.03	N/A
	TXR 2	3.23	2.42	0.045	Good to fair*	N/A	N/A	0.52
*According to Lunne et al (1997)								

10 CONCLUDING REMARKS

Laboratory investigations have been performed to assess the quality of samples obtained using an innovative CPT rig mounted direct-push piston sampler (designated a PPI sampler). The results of CAT scanning suggest that the level of physically observable disturbance in the PPI samplers is less than in a standard U75 Shelby tube. CRS tests indicate that the PPI sample quality is very good to excellent in compression while triaxial tests consolidation phases suggest the sample quality is good to fair. The reduction in quality for triaxial tests might be associated with the trimming process rather than the sampling process. Shear wave velocity measurements show that the small strain stiffness of the PPI samples was within 10% of field measurements that were interpreted as being good quality. There is little difference in laboratory test results between the PPI sample tubes with and without the low adhesion silicone coating. A future development to the system will be inclusion of a grub screw on the piston to relieve suction pressures as the tube is being removed from the piston.

ACKNOWLEDGEMENTS

The first and third authors would like to acknowledge support provided by ARC Centre of Excellence in Geotechnical Science and Engineering at the University of Newcastle, Australia. These partners include Advanced Geomechanics, Coffey Geotechnics and Douglas Partners

REFERENCES

- Australian Standard AS 1289.3.2.1: Soil classification tests-Determination of the plastic limit of a soil-Standard method
Australian Standard AS 1289.3.9.1-2002 : Methods of testing soils for engineering purposes - Soil classification tests - Determination of the cone liquid limit of a soil
- Becker, D.E., Crooks, J.H.A., Ben, K. & Jefferies, M.G. (1987) Work as a criterion for determining in situ and yield stresses in clays. *Canadian Geotechnical Journal*, Vol 24, 549-564.
- Bishop, D. (2010). "Engineering geology of the Richmond River estuary." PhD Thesis, University of Newcastle Australia.
- ISSMFE (1981) International Manual for the Sampling of Soft Cohesive Soils, ISSMFE subcommittee on soil sampling *eds*, Tokyo
- Kelly, R.B. (2013) Australia's first national facility for soft soils testing. *Civil Engineers Australia*, June, 76-78.
- Lunne, T., Berre, T. & Strandvik, S. (1997). Sample disturbance effects in soft low plasticity Norwegian clay. *Proceedings of the Symposium on Recent Developments in Soil and Pavement Mechanics*, Rio de Janeiro, Balkema, Rotterdam, 81-92.
- Pineda, J.A., Arroyo, M., Sau, N., Gens, A. & Pérez, N. (2012) Testing block samples from silty deposits. In. *Proc. Geotechnical and Geophysical Site Characterization 4*, Coutinho & Mayne (eds), Taylor & Francis Group, London, 1815-1823.
- Pineda, J.A., Kelly, R., Bates, L., Sheng, D. and Sloan S. (2013) Effects of pore fluid salinity on the shear strength of a soft clay. In: *Poromechanics V: Proc. 5th Biot Conference in Poromechanics*, ASCE, Hellmich, Pichler and Adam (eds), pp. 1460-1469.
- Viggiani, G. and Atkinson, J.H. (1995) Interpretation of bender element test. *Géotechnique*, Vol 45, No 1, pp. 149-154.